This item was submitted to Loughborough's Research Repository by the author.
Items in Figshare are protected by copyright, with all rights reserved, unless otherwise indicated.

Finite element and experimental modelling of structure-borne vehicle interior noise

PLEASE CITE THE PUBLISHED VERSION

http://media.noisetp.com/filer_public/90/1d/901db970-df4c-4c72-87c9-14c467ef1a73/page_10-26_eng.pdf

VERSION

VoR (Version of Record)

PUBLISHER STATEMENT

This work is made available according to the conditions of the Creative Commons Attribution-NonCommercial-NoDerivatives 4.0 International (CC BY-NC-ND 4.0) licence. Full details of this licence are available at: https://creativecommons.org/licenses/by-nc-nd/4.0/

LICENCE

CC BY-NC-ND 4.0

REPOSITORY RECORD

Georgiev, Vasil B., R.L. Ranavaya, and Victor V. Krylov. 2016. “Finite Element and Experimental Modelling of Structure-borne Vehicle Interior Noise”. figshare. https://hdl.handle.net/2134/20045.

Finite Element and Experimental Modelling of Structure-borne Vehicle Interior Noise

Georgiev, V.B.[1], Ranavaya, R.L.[2], Krylov, V.V.[3]

[1] Research associate, Department of Aeronautical and Automotive Engineering, Loughborough University, Loughborough, Leicestershire, LE11 3TU, UK
[2] Student, Department of Aeronautical and Automotive Engineering, Loughborough University, Loughborough, Leicestershire, LE11 3TU, UK
[3] Professor, Department of Aeronautical and Automotive Engineering, Loughborough University, Loughborough, Leicestershire, LE11 3TU, UK

Abstract

The present paper describes the results of the combined finite element and experimental approach to studying structure-borne vehicle interior noise using a simplified reduced-scale model of a car. The numerical investigation included finite element calculations of structural and acoustic modes as well as frequency response functions for interior acoustic pressure. Experimental tests included measurements of frequency response functions at driver's and passenger's ear positions, when an electromagnetic shaker exciting structural vibrations was located at different places. The effects of engine mass and of boot load on structure-borne interior noise have been investigated as well. Some of the obtained numerical results have been compared with the experimental ones. The obtained reasonably good agreement between them indicates that structure-borne interior noise in the vehicle model under consideration can be predicted and understood rather well. This implies that the proposed combined numerical and experimental approach to studying vehicle interior noise based on using reduced-scale structural models is simple and reliable, and it can be used successfully by noise and vibration engineers for prediction and mitigation of vehicle interior noise on a design stage.

Key words: Vehicle interior noise, Structure-borne noise, Finite element modelling, Experimental modelling.

Introduction

To reduce time and efforts required for analysing and mitigating structure-borne vehicle interior noise it is preferable to undertake most of the associated work on a design stage. Therefore, virtual simulations and different predictive methods become increasingly important in studying vehicle interior noise. They form an integral part of the design and development process as mitigation of intrusive noise leads directly to the enhancement of consumers' perception of product quality [1]. In particular, the tuning of vehicles' acoustic properties to convey distinct characteristics of the brand, especially at low-frequency range, is often considered as an additional motivation for analysing interior noise on this stage [2].

The analysis of structure-borne interior noise can be carried out using different approaches. For a limited number of structures with simple geometry, one can use analytical solutions to structural-acoustic problems [3-5]. This provides a great opportunity for explicit physical interpretation and understanding of the cases considered. In contrast to analytical approaches, the analysis of irregular cavities, representing real car compartments, requires application of different numerical techniques. In the low frequency range, 10-250 Hz, the most common techniques are Finite Element Method (FEM) and Boundary Element Method (BEM), the upper frequency limit reported in the literature being at about 500 Hz [6]. In the high frequency range, above 500 Hz, Statistical Energy Analysis (SEA) is used widely.

E-mail: V.B.Georgiev@lboro.ac.uk, R.Ranavaya@lboro.ac.uk, V.V.Krylov@lboro.ac.uk (corresponding author)

From the very early stage of vehicle interior noise studies, the attention has been paid to developing of a complete strategy of interior noise reduction on a design stage. One of the first works of this kind has been carried out by Nefske et *al.* [7] who computed acoustic modes and interior noise levels using FEM, when structural vibrations were supposed to be known. At a later stage, Sung and Nefske [8] predicted vehicle interior noise and identified noise sources for a coupled system 'vehicle structure – acoustic interior'.

Although the approaches based on detailed numerical calculations have achieved satisfactory levels of accuracy in predicting interior structural-acoustic response, they are not much helpful in understanding physical mechanisms behind the problem, which would be of great importance for predicting the behaviour of similar but slightly modified vehicle structures. Therefore, there remains the scope for developing a new combined numerical and experimental approach to studying vehicle interior noise based on using simplified reduced-scale vehicle models. Such models can be easily used for different laboratory measurements, and, due to their simplicity, they can assist in better understanding the physics of structure-borne interior noise, in particular its dependence on different parameters of vehicle structures and interior cavities.

Note that a number of simplified and reduced-scale models have been used already by a number of authors for theoretical and experimental investigations of some aspects of vehicle interior noise. For example, purely acoustic experiments have been conducted on scale replicas of vehicle interiors, with walls described by rigid boundary conditions [9, 10]. In particular, in the example described by Lee *et. al.* [9], the model was a 1:2 scale replica of the passenger compartment of a saloon car, whereas Gorman *et. al.* [10] simplified their vehicle models to equivalent rectangular and octagonal cavities having the same volume as the actual enclosure. Recently, the well known structural-acoustic model – a rigid rectangular box with one flexible wall - was investigated again to demonstrate a new hybrid method for simulating the so-called 'boom noise' and identifying the parameters that affect its generation [11]. In addition to the above, some new types of simplified and reduced-scale structural-acoustic models have been suggested for studying vehicle interior noise both theoretically and experimentally [12-16]. In particular, one of such simplified models contained a non-circular cylindrical shell as its flexible element that could be described both analytically and numerically.

The present paper describes the results of the combined finite element and experimental approach to studying structure-borne vehicle interior noise based on using simplified reduced-scale vehicle models. In the framework of this approach, a new reduced-scale vehicle model of intermediate complexity has been designed and tested both numerically and experimentally. Some of the results described in this paper have been published in the authors' earlier paper [17].

A number of finite element calculations of structure-borne vehicle interior noise have been carried out using finite element packages MSC.Nastran and MSC.Patran. Experimental tests included measurements of structural-acoustic frequency response functions at driver's and passenger's ear positions, when an electromagnetic shaker was located at different parts of the vehicle model structure, thus simulating different sources of vehicle structural vibrations. In addition to these, the effects of engine mass and of boot load on generated structure-borne interior noise have been investigated in detail. As a simple measure of interior noise reduction in the reduced-scale vehicle model under consideration, the effect of sound-absorbing seats made of foam material has been tested experimentally. The results of some of the finite element calculations have been compared with the relevant experimental measurements.

1. Reduced-scale Vehicle Model and Experimental Setup

The 1:4 reduced-scale vehicle model considered in the present paper is shown in Fig. 1. Although this model has a rather complex geometrical form, it is still simple enough to enable studying the effects of different model parameters on generated structure-borne vehicle interior noise using laboratory measurements and not time-consuming finite element calculations.

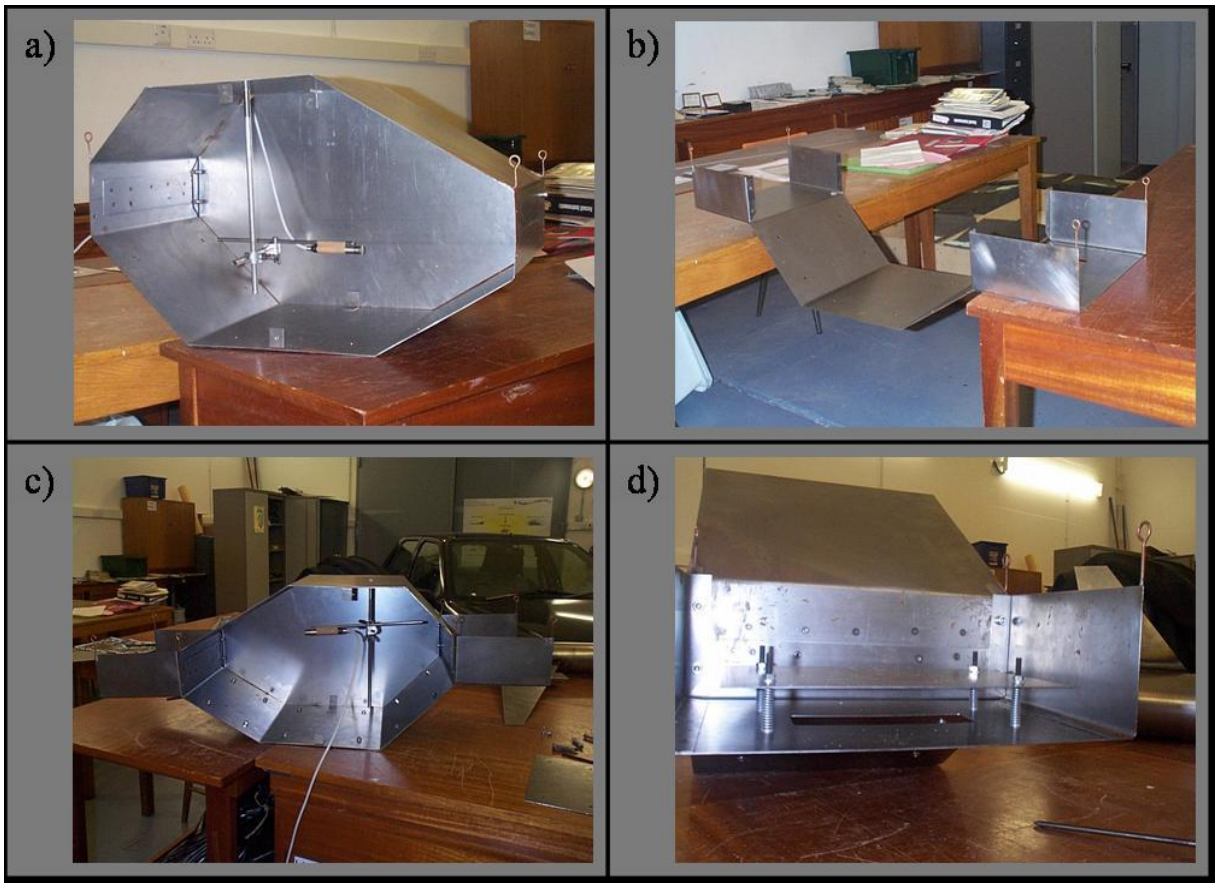

Fig. 1. Views of the reduced-scale vehicle model and of its different parts: a) the cavity section, b) the under-cavity section, c) the whole model, and d) the engine section

The model consists of two main parts: the cavity and under-cavity sections (note that the cavity section can be considered and investigated separately as an independent model of vehicle cabin). Two side walls are attached to the cavity section by means of six bolts. The under-cavity part includes boot and engine sections, the latter one being represented by a plate joined to the under-cavity part by four bolts and springs that can be considered as engine mounts. All model parts have been built of metal sheets of 1 mm thickness and spot welded where necessary. Both parts (cavity and under-cavity) can be joined together by bolts to form a more complex whole vehicle model, which is of primary interest in this investigation. Detailed pictures of the model's components can be seen in Fig. 1. Note that in the process of scaling of structural acoustic models *all* acoustic and structural dimensions must be scaled, including structural thickness [15].

In order to simulate the boundary conditions on the bottom of the model vehicle that would be similar to those for real vehicles the model was fixed by four bolts to two wooden

beams that in turn were firmly joined by clamps to a massive foundation (a laboratory table). This type of attachment of the model corresponds to the so-called "grounded" boundary conditions.

All experimental measurements of structure-borne interior noise in the above-mentioned reduced-scale vehicle model have been carried out in the Noise and Vibration Laboratory at the Department of Aeronautical and Automotive Engineering at Loughborough University. The measurement data were recorded using an HP 3566 FFT analyzer. The excitation signal, a continuous white noise, was generated by the analyzer and transmitted to a Ling Dynamic Systems 200 series electromagnetic shaker by means of an amplifier ENDEVCO Model 27218. The amplitude of the driving force from the shaker was measured using a sample mass and accelerometer, and it was evaluated as 2.8 N. For acoustic frequency response measurements, a Bruel & Kjaer Type 4133 microphone was used. Its signal was amplified by a Dual Microphone Supply Type 5935. A mechanical clamp enabling longitudinal and lateral motion inside the cavity assured the positioning of the microphone in a desired location. The Bruel & Kjaer Type 2635 charge amplifier was used to enhance the signal from a force transducer Bruel & Kjaer Type 8200. The transducer's reference sensitivity was 3.85 pc/N, and its weight was 21g.

2. Results of the Finite Element and Experimental Studies

2.1. Numerical Analysis of Structural-acoustic Normal Modes.

The structural-acoustic normal mode analysis has been conducted using FEM techniques for two different cases. In the first case, only the cavity model was considered, whereas in the second case the whole model, i.e. cavity plus under-cavity, was under examination. The interior cavity was the same for both models, and the acoustic numerical model for it was built using 3420 CHEXA and 44 CPENTA acoustic finite elements and in total 4147 nodes. The structural model of the cavity section was constructed using 1342 CQUAD structural finite elements and 1458 nodes. The whole structural model, including cavity and under-cavity, consists of 1662 CQUAD structural elements and 1863 nodes. The normal mode analysis was performed using modal analysis reduction for the first 300 modes only. In contrast to the model presented in [14], the present two models have higher numbers of degrees of freedom. There are about 293 natural frequencies in the range from 0 to 1.7 kHz.

The results of the numerical calculations show that structural normal modes of the first model (cavity) include local modes for individual panels and global modes that spread almost over all panels (see Fig. 2). The analysis shows that the structure of the cavity model can not be broken up into different regions in specific frequency ranges, as it was possible for the QUASICAR model [14]. The reason for that is that the constitutive panels have nearly the same modal parameters and their natural frequencies are roughly in the same frequency range. However, the side walls demonstrate a more specific vibration behaviour due to their rather loose attachment to the main structure, that presumes less restriction compared to other panels. Most of the normal modes of the side walls can thus be defined as local. Participation of the side walls' normal modes in global structural displacement of the model can be only observed at certain frequencies.

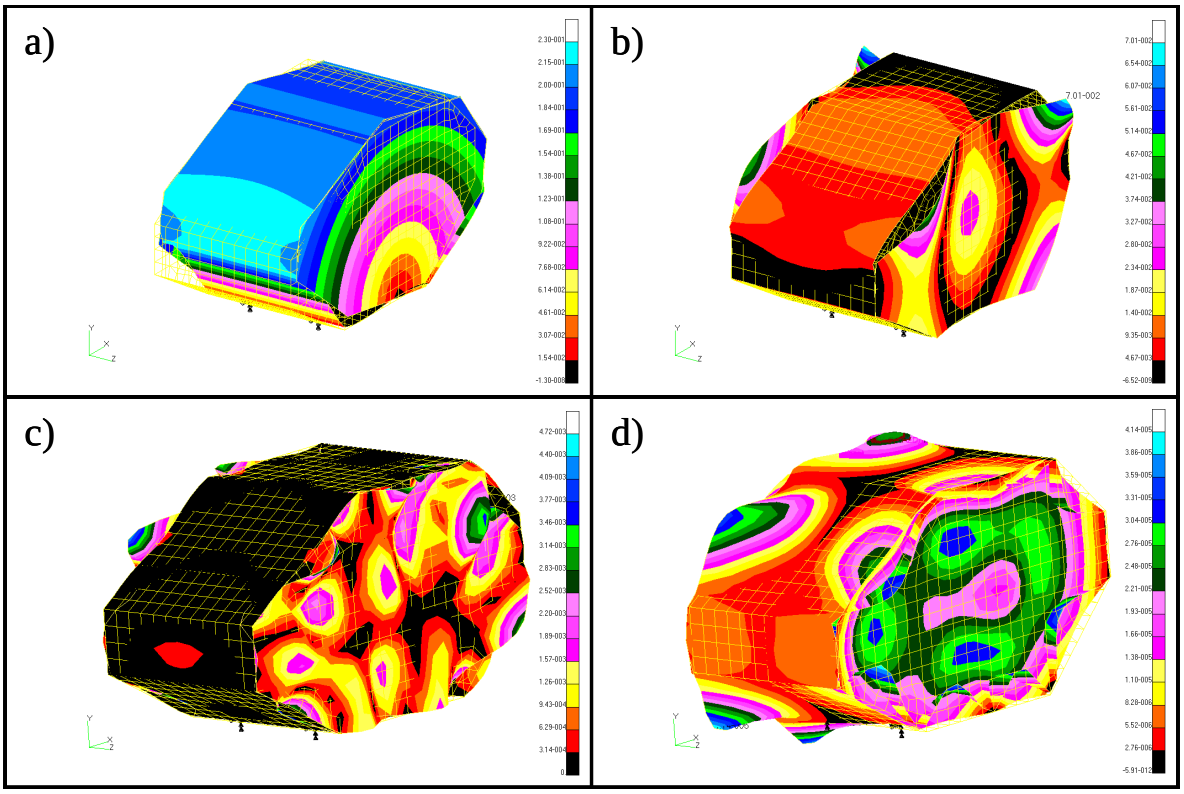

Fig. 2. Structural normal modes of the cavity model at: a) 11.525 Hz, b) 59.586 Hz, c) 325.07 Hz, and d) 560.65 Hz.

In contrast to the side walls, the main structure exhibits more complex and obscure vibration behaviour, as can be seen in Fig. 2. The constitutive panels take part in both the global and local structural motions. In the low frequency range, the global modes are predominant, whereas in the high frequency range the local modes of different panels become readily distinguishable.

An interesting feature of the current model is the effect of welded joints along edges of the main structure (in comparison with simply-supported boundary conditions that have been implemented in the earlier investigated reduced-scale model QUASICAR [14]). In particular, the presence of welded joints facilitates the appearance of global modes at very low frequencies, as it can be seen in Fig. 2(d). Note in this connection that global modes of the QUASICAR model (that contained a non-circular shell as a vibrating structure [14]) appeared only at relatively high frequencies, above 1 kHz.

The structural-acoustic normal mode analysis of the whole model, which included cavity plus under-cavity sections, shows some resemblance to the first model, but demonstrates certain specific features as well (see Fig. 3). Again, in this case the side walls are involved in many normal modes in the whole frequency region.

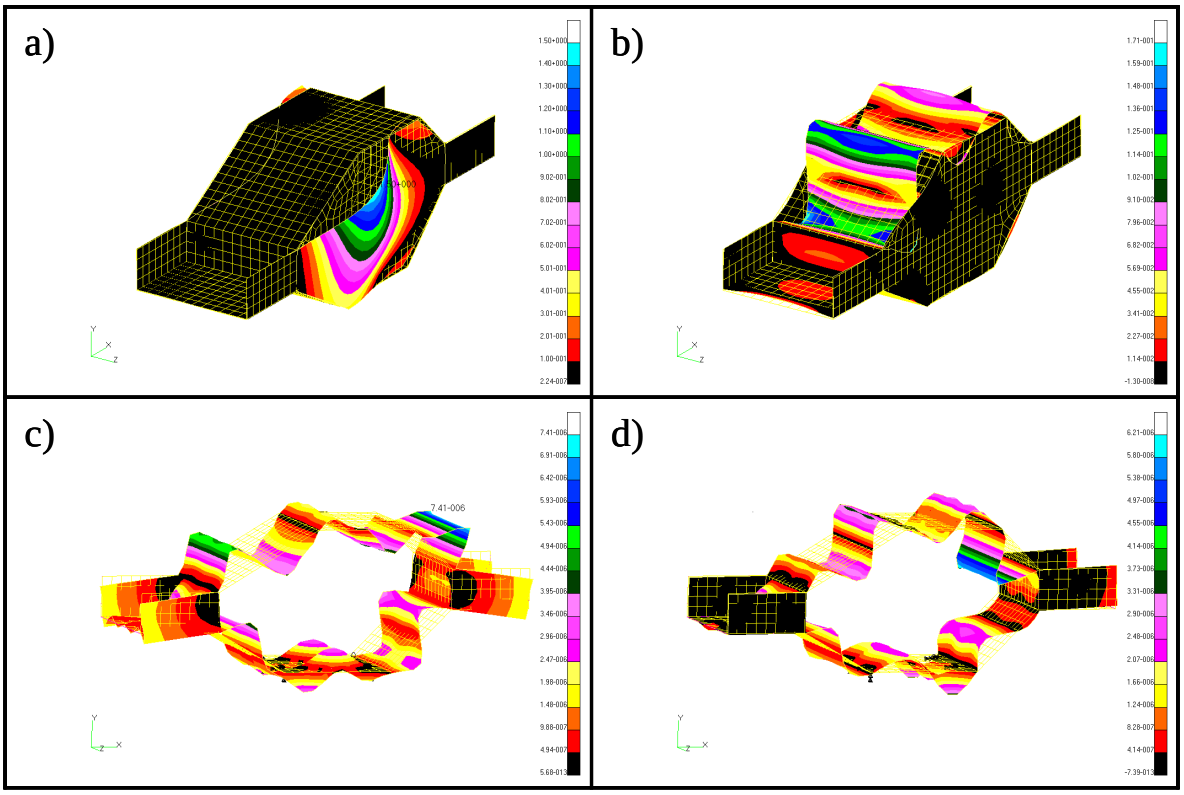

Fig. 3. Structural normal modes of the whole model at: a) 21.87 Hz, b) 136.91 Hz, c) 1399.20 Hz, and d) 1629.6 Hz ; in the last two pictures the side walls are not shown for clarity

The structural behaviour of the whole model is also affected by boot and engine sections which are firmly attached to the cavity and side walls by bolts. This is why, the first resonant peak for this model exists at a higher frequency, 21.87 Hz, whereas in the first model the fundamental frequency is 11.525 Hz (see Fig. 2(a), Fig. 3(a) and Table 1).

Table 1
First five structural and acoustic natural frequencies of the cavity model and of the whole model

Cavity model: structural frequencies, Hz	Whole model: structural frequencies, Hz	Hard-wall model: acoustic frequencies, Hz	Cavity model: acoustic frequencies, Hz	Whole model: acoustic frequencies, Hz
1	2	3	4	5
11.525	21.87	326.66 (1, 0, 0)	325.07	327.51
15.52	28.759	529.22 (0, 1, 0)	536.00	538.44
23.486	31.498	553.74 (0, 0, 1)	560.65	555.18
26.626	33.28	584.46 (2, 0, 0)	589.45	588.24
28.255	36.394	642.92 (1, 0, 1)	648.76	646.53

The boot and engine sections, particularly their vertical sides, appear to be quite loose; they are first involved in the normal mode at 42 Hz (see Fig. 3(b)) and stay active in the whole frequency range. Surface displacements of the upper three cavity panels look similar to

the case of the first model (see Fig. 2(d) and Fig. 3(e)). However, the global modes, which they are involved in, are realized at higher frequencies (Figs. 3(e) and 3(f)), as compared to the cavity model only. The reason for that could be the double thickness of the bottom cavity's panels due to the firm attachment of the under-cavity to the cavity.

The bottom panels of the cavity, in case if the whole model is considered, have different modal parameters due to the double thickness, and their surface displacements differ completely from the displacements of the first model. The local fundamental frequency of the bottom plate is 64.369 Hz for the first model and 196.98 Hz for the second model. In the low and medium frequency ranges this part of the whole model is structurally almost 'silent', and its structural activity starts at higher frequencies. This behaviour is similar to the structural dynamics of the modified QUASICAR model with increased thickness of the bottom panel [14]. In both cases the additional thickness suppresses structural activity of the treated panels in a certain frequency range, which gives a simple demonstration of this method of passive structural vibration control.

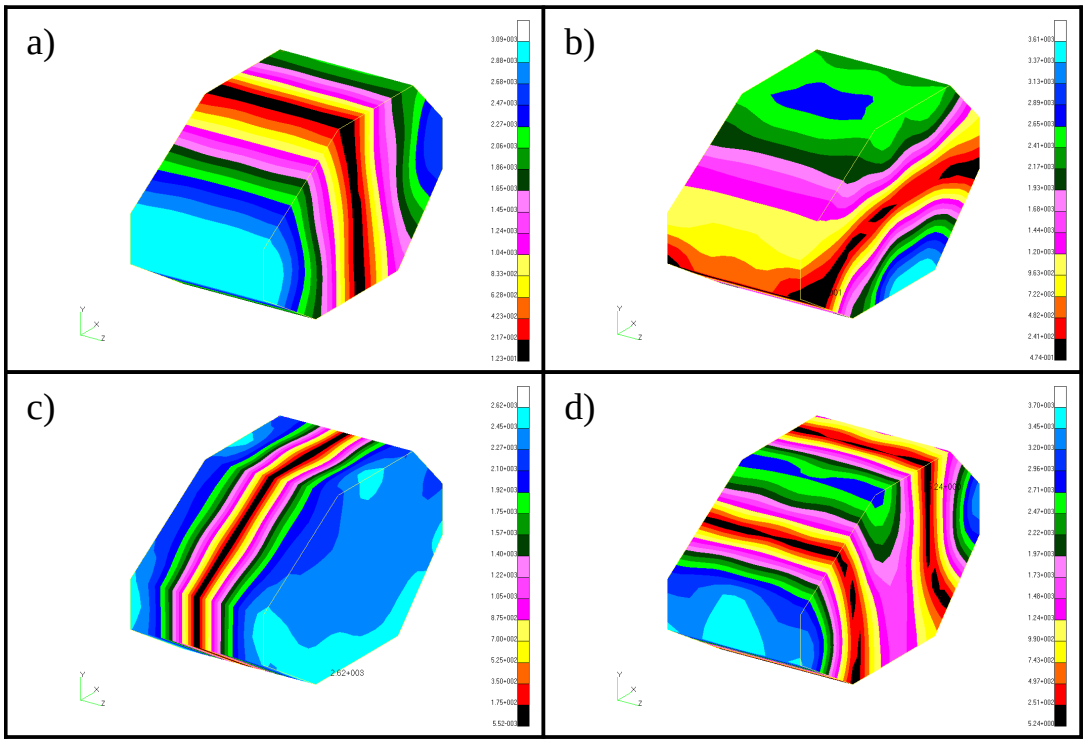

Fig. 4. First four acoustic normal modes of the cavity at: a) 327.51 Hz, b) 529.57 Hz, c) 555.18 Hz, and d) 587.01 Hz.

In Table 1, Columns 3, 4 and 5, one can see the values of the first five acoustic resonant frequencies calculated for the acoustic model with rigid walls, for the cavity model and for the whole model respectively (calculations for the two latter models took full structural-acoustic coupling into account). The first four acoustic modes can be seen in Fig. 4. Obviously, the different boundary conditions for each model affect the acoustic resonant peaks of the cavity, slightly shifting their frequencies. Observations of the sets of acoustic resonances for these three models did not show any specific patterns. The only difference is that the resonant peaks of the latter two models appear to be higher than those of the first one, as it can be seen in the Table 1. Therefore, one can not say how exactly the additional under-cavity body mass

influences the acoustic normal modes of the cavity. However, the change in the frequency sets from the case of the first model to the latter two is readily noticeable, reflecting the effect of full structural-acoustic coupling.

2.2. *Experimental and Numerical Analysis of Frequency Response Functions.*

The frequency response functions (FRF's) have been investigated for both models using both numerical and experimental techniques. In total 83 experimental tests and 48 numerical simulations have been carried out. The covered frequency range was between 0 and 1.6 kHz, which for full size models corresponds to the range 0 - 400 Hz. A resolution of one point per 1 Hz for both numerical and experimental tests was adopted.

For all experimental tests the models were attached firmly to tables using the wooden beams mentioned in Section 2. Because the masses of the tables were comparable to the masses of the models, their frequency responses could be affected by tables' modal parameters. This is why heavy weights were placed on the top of the tables to assure proper grounded boundary conditions. The microphone was placed inside the cavity at the required point of observation. Two points in the interior cavity were of particular interest, the driver's ear position (0, -90, 70) cm and the passenger's ear position (250, -90, 70) cm, in respect to the front upper left corner of the cavity.

2.2.1. *Effect of the Shaker and Microphone Positions.*

Both models have been examined in a number of structural-acoustic tests, including measurements of acoustic response at driver's and passenger's ear positions, whereas the electromagnetic shaker was located at five different positions at the bottom plate, thus simulating dynamic forces due to road roughness. Obviously, the locations of the shaker and of the microphone strongly influence the acoustic response. Since frequency responses of both the structure and the fluid can be represented as infinite sums of their normal modes, then, if the driving force coincides with a certain nodal point of some structural normal modes, the structure will not be excited properly in the corresponding frequency range. The same situation can be considered for the location of a microphone. If a microphone (receiver) is located in the vicinity of a nodal point of some acoustic normal modes, then the sound pressure response will be reduced.

In principle, the location of the driving force and of the microphone could be used for optimal reduction of perceived interior noise. However, the practical effect of such an approach is arguable. The location of the driving force or of the microphone may coincide with nodal positions for some modes, but in the same time it might be in anti-nodal positions for some other normal modes. This means that noise reduction can be achieved at a certain frequency range, but there can be an increase beyond this range.

Figure 5(a) shows the results of finite element calculations of the effects of different locations of the driving force with the amplitude of 2.8 N on the acoustic responses. In particular, one can note that in test 3 the force does not excite properly some of the first normal modes. This is why in the low frequency range the acoustic response is reduced in comparison with test 1. On the other hand, in the high frequency range the location of the driving force at the left front position excites the normal modes in this area, and the acoustic response is higher than that in test 1.

Figure 5(b) presents the acoustic responses at driver's (test 13) and passenger's (test 26) ear positions taken for the whole model, when the driving force was located at the left front position of the bottom plate.

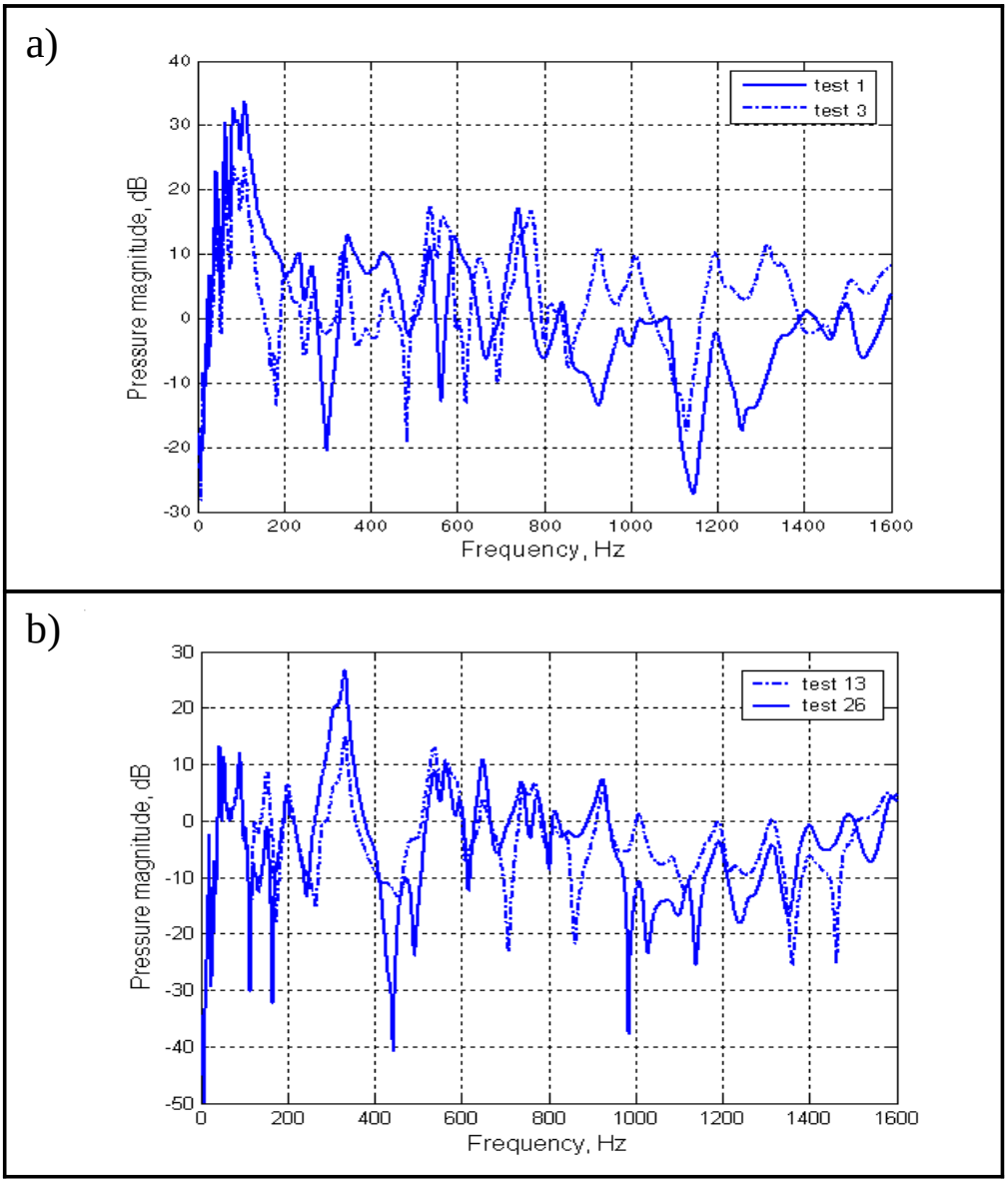

Fig. 5. Structural-acoustic pressure FRF's for different locations of a shaker (a) and a microphone (b): test 1 - central position of a shaker (solid curve), test 3 - left front position of a shaker (dash-dotted curve); test 13 - driver's ear position of a microphone (dash-dotted curve), and test 26 - passenger's ear position of a microphone (solid curve).

Similarly to the analysis above, the sound pressure readings shows some frequencies where the resonant peaks are considerably reduced, as at 320 Hz. In this case the sound perception at the driver's ear position is reduced almost by 10 dB compared to the passenger's ear positions. However, at 1000 Hz the reduction is again about 10 dB, but this time it is for a passenger's ear position.

2.2.2. *Comparison of Experimental and Numerical Results*.

The purpose of comparison between the experimental and finite element results in the present work was to evaluate to what extent the proposed experimental and numerical

approaches are reliable and precise. Figure 6 shows sound pressure responses for experimental and finite element simulations for the whole model.

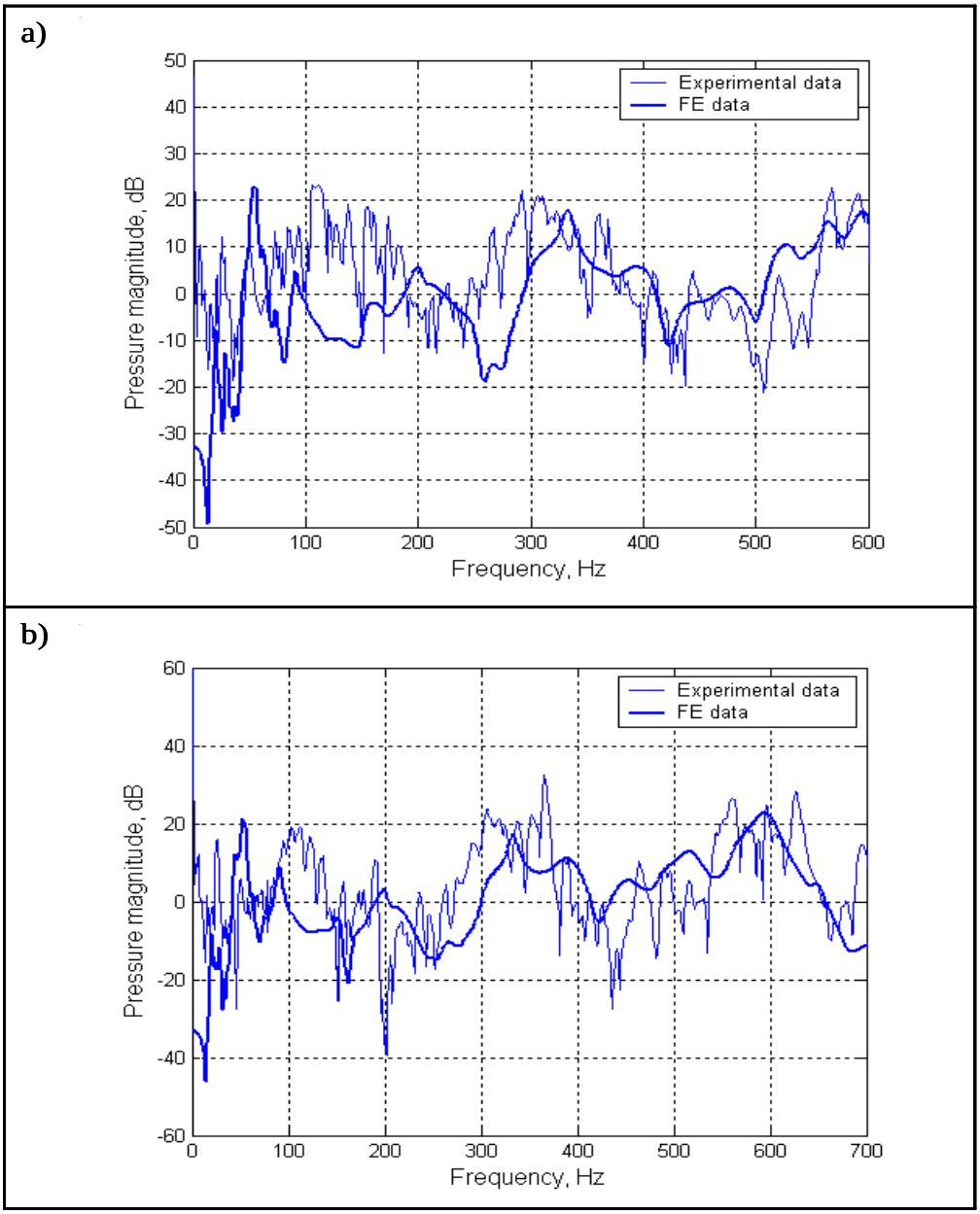

Fig. 6. Structural-acoustic pressure FRF's of the whole model obtained experimentally (single thickness curves) and by finite element calculations (double thickness curves) for a shaker placed at the front right position in the engine section (a) and at the back right position in the boot section (b).

The electromagnetic shaker with the force amplitude of 2.8 N was placed at the front right position in the engine section (Fig. 6(a)) and at the back right position in the boot section (Fig. 6(b)). Finite element mesh was consistent with the frequency limit of interest about 500 Hz; with about six finite elements per wavelength. In the FEM frequency response analysis, a resolution equal to one point per 1 Hz was used, which was the same as in the experimental testing.

One can see that there is a reasonably good overall coincidence between the experimental and FEM data. This proves that both FEM calculations and experimental measurements are reliable enough to be used either together or separately for studying structure-borne vehicle interior noise in simplified reduced-scale models under consideration. Therefore, in subsequent sections of this paper either numerical or experimental investigations will be used to analyse some specific interesting cases of generation of structure-borne vehicle interior noise.

2.2.3. *Effect of the Engine and Boot Masses*.

The effects of additional masses placed in the engine and boot sections have been examined in experimental tests 57 to 75. For all of the tests the microphone was located at driver's ear position and the electromagnetic shaker was moved to different positions from left to right in the engine and boot sections. However, no matter where the position of the shaker was, the sound pressure responses showed some common features for all tests. Since the engine mass was separated from the main model structure by elastic elements, its effect on acoustic response was barely detectable, as it can be seen in Fig. 7(a). The graphs show the pressure magnitude without the engine mass (test 66) and with the engine mass equal to 5 lb (test 67), where the shaker was placed at the middle left position of the boot plate. Obviously, the presence of elastic elements between the engine mass and the structure simulated engine mounts.

Although the resulting tests pointed out clearly that the elastic elements suppresed successfully the effects of engine mass, it must be mentioned that in the present experiment the engine was modelled only as a mass unit, but not as a source of vibration. In practice, however, the engine can experience its own vibrations, e.g. due to rotating imbalance. These can result in dynamic forces applied to the vehicle structure that could cause additional structural vibrations. Such aspects though were beyond the scope of this investigation.

Figure 7(b) shows the graphs of sound pressure response in the case of absence of additional mass in the boot section (test 66) and in the case of presence of the additional boot mass equal to 5 lb (test 68). The additional boot mass was placed freely in the boot section, without any elastic elements, thus simulating the effect of luggage placed in the boot in real practical situations. It is seen from Fig. 7(b) that the resonant peaks are slightly shifted, in comparison with Fig. 7(a), and there are some changes in their amplitudes. Particularly, in the low frequency range the maximum peak is shifted from about 90 Hz to 160 Hz, whereas in the high frequency range, above 1 kHz, the acoustic response is slightly reduced.

Although the overall sound levels in the case of presence of the boot mass remain aproximately the same, the experiments demonstrate the influence of such mass, e.g. luggage, on the frequency contents of interior noise. In particular, the boot masses can cause rather large resonant peaks at certain frequencies that would annoy the driver and passengers in the car compartment. For example, in the present work such a peak can be observed in Fig. 7(b) between 800 and 900 Hz.

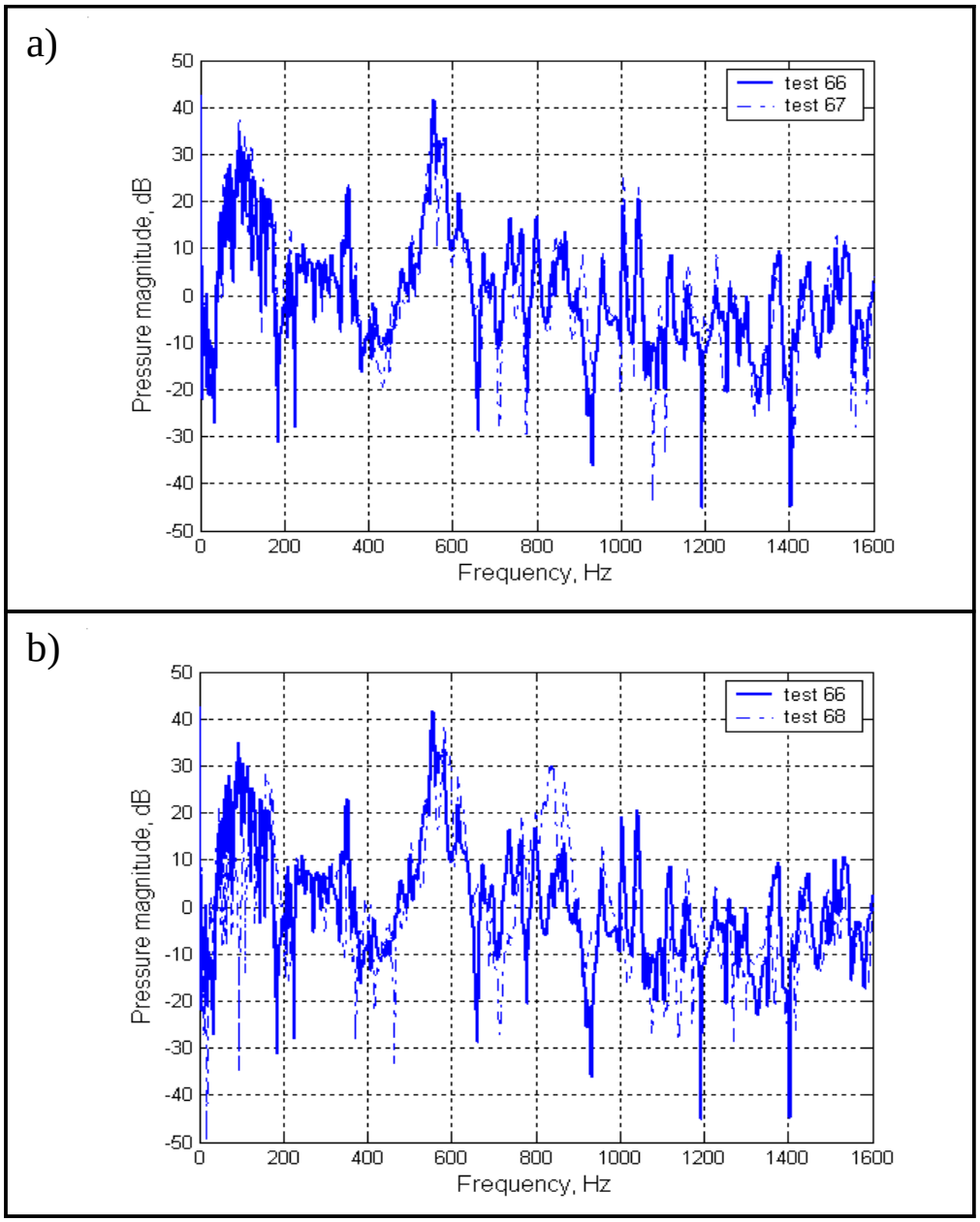

Fig. 7. Effects of the engine mass (a) and of the boot mass (b) on structural-acoustic FRF's: test 66 - no engine and no boot masses (solid curve), test 67 – with the engine mass, but no boot mass (dash-dotted curve); and test 68 - with the mass in the boot, but no engine mass (dash-dotted curve).

2.2.4. *Effect of Sound Absorbing Seats.*

The effect of seats made of foam has been studied by experimental testing including tests from 30 to 57 for both models. It was expected that the acoustic response would be reduced because of the seats' being made of sound absorbing material such as foam. Indeed, this anticipation was found to be correct to some extent. Adding the two seats, that are shown in Fig. 8, could affect the sound pressure response in two ways. First of all, according to the analytical expressions for interior sound pressure in some simple models, the generated noise

level is inversely proportional to the air volume (see e.g. [12]). Thus, any decrease of actual interior volume could lead to the increase in the acoustic response of the enclosed cavity. On the other hand, the model seats considered are made of sound absorbing material (foam), and this would increase the acoustic energy dissipation, thus reducing the sound pressure response. Therefore, it is the balance of these two opposite effects that defines the actually observed acoustic response in the models with added foam seats.

The measured acoustic responses for all tests in this section show that in the low frequency range the effect of added seats is negligible, whereas in the high frequency range the reduction of sound pressure is readily noticeable.

Fig. 8. View of the interior of the whole model with the inserted foam seats.

In Fig. 9, the sound pressure responses are presented for two different locations of electromechanical shaker, (a) the shaker is placed at the front-left position on the bottom plate, and (b) the shaker is at the front-right position on bottom plate. In Fig. 9(a), test 13 corresponds to the model without seats, whereas test 35 was carried out for the model with added seats. And respectively in Fig. 9(b), test 14 corresponds to the model without seats, and test 37 – to the model with seats.

Obviously, the seat-related reduction of interior volume is a constant value causing the increase in sound pressure that is independent of frequency. On the other hand, the foam seats dissipate the acoustic energy, which is done most efficiently at higher frequencies. Thus, the observed very small change in acoustic pressure in the low frequency range can be attributed to the balance between the volume change and low-frequency foam dissipation, whereas the noticeable reduction of the response at higher frequencies is mainly due to energy dissipation by foam seats.

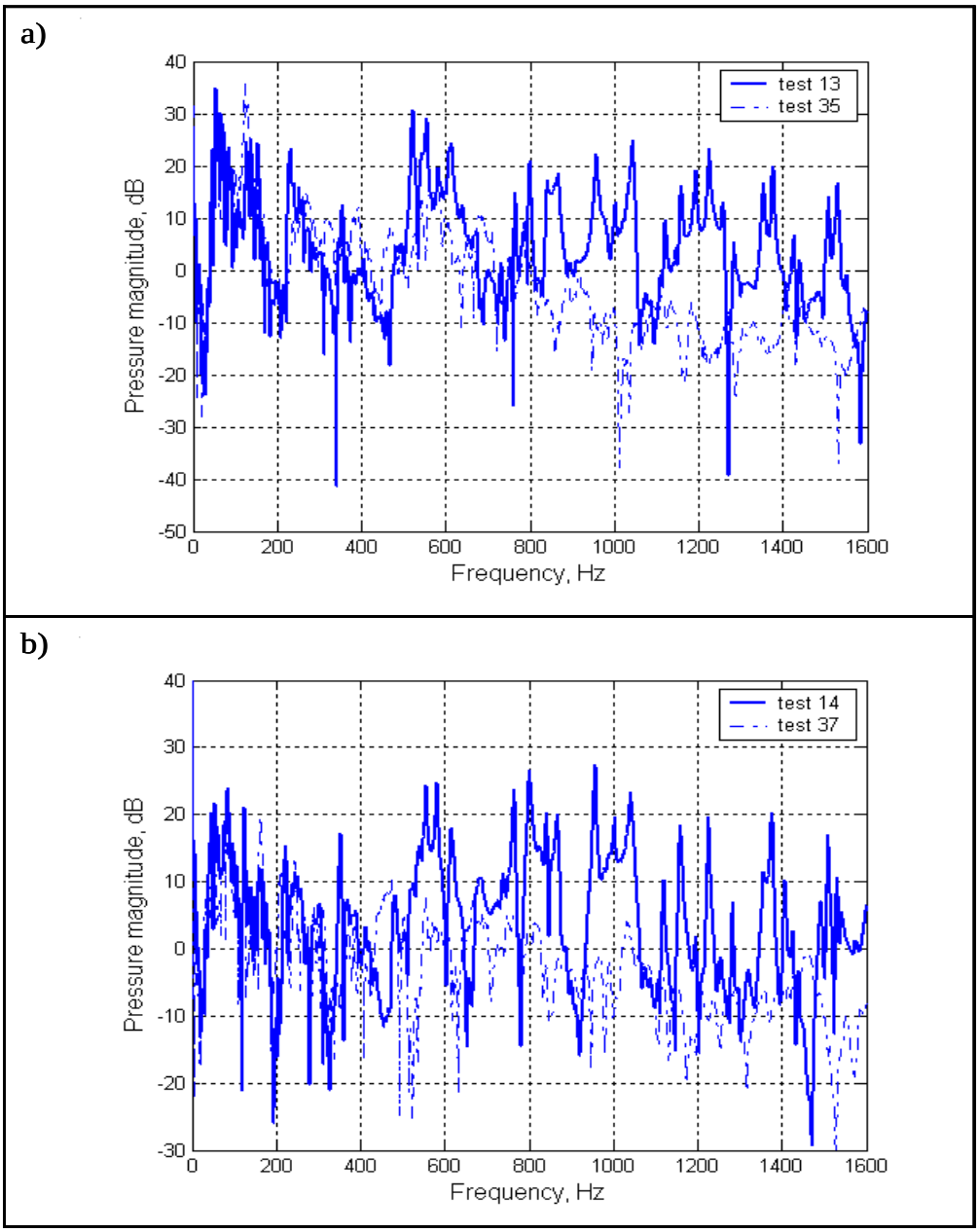

Fig. 9. Effect of foam seats on structural-acoustic FRF's for different positions of a shaker: a) left front position – test 13, no seats (solid curve) and test 35, with seats (dash-dotted curve); b) right front position – test 14, no seats (solid curve) and test 37, with seats (dash-dotted curve).

2.2.5. *Comparison between Acoustic Responses of the Cavity and of the Whole Model.*

In this section, the measured structural-acoustic responses of the cavity model and of the whole model, including the cavity and under-cavity sections) are discussed. In spite of the fact that the interior cavity is the same for both models, the pressure magnitudes behave differently due to the structural modifications associated with the whole model. First of all, the mass of the whole model structure is substantially larger, and the thickness of the three bottom panels of the cavity is doubled. Secondly, the boundary conditions for the cavity model are applied to four points lying in the horizontal bottom plate, whereas for the whole model they are applied to the two points lying in the engine section and to the two points in

the boot section. Thus, the distance between these two sets of points, which simulates a vehicle base, is much larger for the whole model than for the cavity model.

Figure 10 shows the comparison of the two sets of data for the above two models.

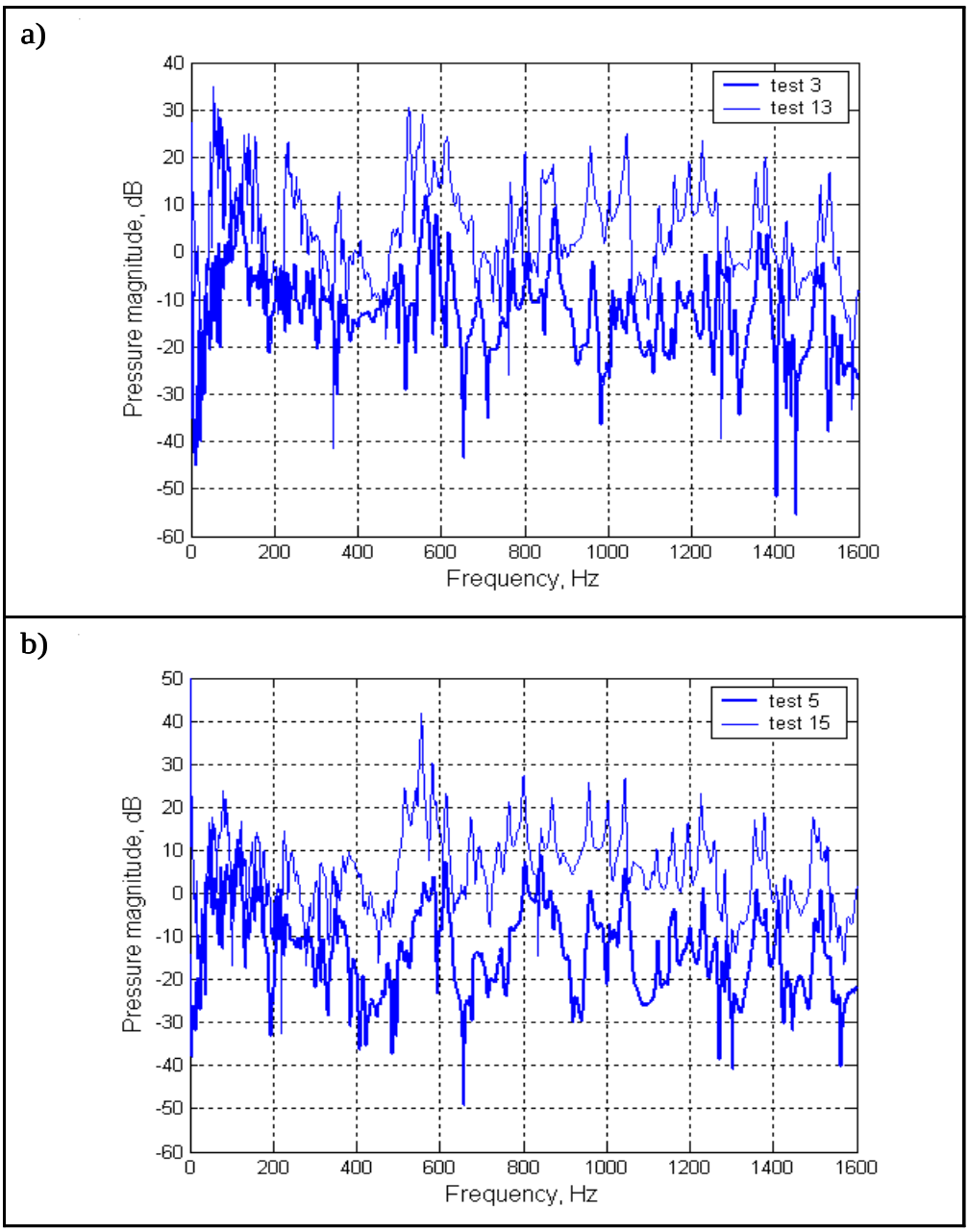

Fig. 10. Comparison between structural-acoustic FRF's of the whole model (single curves) and of the cavity model (double curves) at two positions of the shaker: a) front left position and b) back right position

For the first set, shown in Fig. 10(a), test 3 and test 13 correspond respectively to the cavity and to the whole model. In this case the shaker was placed at the left front position on the bottom cavity plate - for the cavity model, and at the engine section - for the whole model.

The second set, shown in Fig. 10(b), represents test 5 and test 15 associated respectively with the cavity and with the whole model, and the shaker was located at the back right position, correspondingly on the bottom plate and in the boot section. Both sets of data show

that the acoustic response in the whole model is significantly increased in the entire frequency range. In Fig. 10(a), one can see more clearly the change in the first structural resonance due to the structural modification associated with the transition from the cavity to the whole model.

One can assume that the larger base of the whole model makes it a bit looser, particularly in the area of the cavity. This could be a possible explanation for the observed higher sound levels in this model. Also it can be seen that some of the resonant peaks coincide completely in both graphs, which is not surprising, keeping in mind that the interior cavity is the same for both models.

3. Conclusions

In the present paper, the results of the combined finite element and experimental studies of structure-born interior noise in the two simplified vehicle models have been reported. In particular, the normal mode analysis of the models and some of their frequency responses have been carried out by finite element simulations. A large number of experimental tests have been conducted. Some of them have been compared with the results of finite element simulations. The observed reasonably good agreement between the experimental and numerical results can be considered as confirmation of the acceptable precision and reliability of the numerical and experimental procedures used in the present work.

The effects of different factors on frequency response functions of both models have been investigated both experimentally and numerically.

In particular, it has been demonstrated, as expected, that the positions of the shaker and of the microphone change significantly the sound pressure response in cases when they are placed at a node or anti-node of respective structural or acoustic normal modes.

It has been shown that the effect of engine mass can be significant or negligible, depending on the elastic elements, whereas the boot mass can be responsible for a noticeable resonant peak at a certain frequency.

The effects of sound absorbing seats (made of foam) on the interior noise reduction in the vehicle model under consideration have been investigated experimentally. It has been demonstrated that the presence of foam seats considerably reduces the sound pressure response, and their noise reducing efficiency increases in the high frequency range.

The whole investigation described in this paper has confirmed the usefulness of the proposed combined numerical and experimental approach based on using simplified reduced-scale models. These models can be sufficiently complex in order to take into account the effects of some important vehicle components (such as engine, boot, seats, etc.), but they are still simple enough to be investigated and understood easier than real size vehicle prototypes. In other words, such simplified reduced-scale models can bridge the existing gap between the simplest analytical models made of rectangular boxes and the full-scale commercial computer models used in automotive industry. The proposed combined finite element and experimental approach to studying structure-borne vehicle interior noise based on reduced-scale models can be used by car manufacturers and noise and vibration engineers for prediction and mitigation of vehicle interior noise on a design stage.

References

1. Pozar, M., Cook, H.E., "On determining the relationship between vehicle value and interior noise", *SAE paper 980621*, 1998.

2. Bisping, R., Giehl, S., Vogt, M., "A standardised scale for the assessment of car interior sound quality", *SAE paper 971976*, 1997.

3. Pretlove, A.J., "Free vibrations of a rectangular panel backed by a closed rectangular cavity", *Journal of Sound and Vibration*, vol. 2, pp. 197-209, 1965.

4. Pretlove, A.J., "Forced vibrations of a rectangular panel backed by a closed rectangular cavity", *Journal of Sound and Vibration*, vol. 3, pp. 252-261, 1966.

5. Lyon, R.H., "Noise reduction of rectangular enclosures with one flexible wall", *Journal of the Acoustical Society of America*, vol. 35, pp. 1791-1797, 1963.

6. Lim, T.C., "Automotive panel noise contribution modelling based on finite element and measured structural-acoustic spectra", *Applied Acoustics*, vol. 60, pp. 505-519, 2000.

7. Nefske, D.J., Wolf Jr, J.A., Howell, L.J., "Structural-acoustic finite element analysis of the automobile passenger compartment: a review of current practice", *Journal of Sound and Vibration*, vol. 80, pp. 247-266, 1982.

8. Sung, S.H., Nefske, D.J., "A coupled structural-acoustic finite element model for vehicle interior noise analysis", *Journal of Vibr., Acoust., Stress, Reliab. Design: Trans. of the ASME*, vol. 106, pp. 314-318, 1984.

9. Lee, W.G., Park, S.K., Suh, M.W., "A study on active noise control using the half scaled compartment cavity model", *SAE paper 940606*, 1994.

10. Gorman, R., Krylov, V.V., "Investigation of acoustic properties of vehicle compartments using reduced-scale simplified models", *Proceedings of the Institute of Acoustics*, vol. 26(2), pp. 37-48, 2004.

11. Rashid, R., Langley, R.S., "A hybrid method for modelling in-vehicle boom noise", *Proceedings of the International Conference on Noise and Vibration Engineering (ISMA 2004)*, Leuven, Belgium, pp. 3487-3500, 2004.

12. Krylov, V.V., "Simplified analytical models for prediction of vehicle interior noise", *Proceedings of the International Conference on Noise and Vibration Engineering (ISMA 2002)*, Leuven, Belgium, vol. 5, pp. 1973-1980, 2002.

13. Krylov, V.V., Walsh, S.J., Winward, R.E.T.B., "Modelling of vehicle interior noise at reduced scale", *Proceedings of the International Conference "Euronoise 2003"*, Naples, 2003 (on CD).

14. Georgiev, V.B., Krylov, V.V., Winward, R.E.T.B., "Finite element analysis of structural-acoustic interaction in simplified models of road vehicles", *Proceedings of the Institute of Acoustics*, vol. 26(2), pp. 25-36, 2004.

15. Georgiev, V.B., Krylov, V.V., Winward, R.E.T.B., "Simplified modelling of vehicle interior noise: Comparison of analytical, numerical and experimental approaches", *Journal of Low Frequency Noise, Vibration and Active Control*, vol. 25(2), pp. 69-92, 2006.

16. Georgiev, V.B., Krylov, V.V., "Finite element study of the effect of structural modifications on structure-borne vehicle interior noise, *Journal of Vibration and Control*, vol. 15(4), pp. 483-496, 2009.

17. Georgiev, V.B., Ranavaya, R.L., Krylov, V.V., "Experimental and numerical investigation of structure-borne interior noise in a simplified vehicle model", *Proceedings of the Institute of Acoustics*, vol. 26(1), pp. 412-421, 2006.